Marzo, A. (2020). Standing waves for acoustic levitation. En D. Zang (Ed.), Acoustic Levitation (pp. 11-26). Springer Singapore. https://doi.org/10.1007/978-981-32-9065-5_2

# Chapter 2. Standing Waves for Acoustic Levitation

Asier Marzo *(asier.marzo@unavarra.es)*

*UpnaLab, Public University of Navarre, Pamplona 31006, Spain.*

## 1. INTRODUCTION

Sound is a mechanical wave transporting momentum capable of exerting forces on objects as a consequence of the acoustic radiation force [1,2,3,4]. If the forces that act on an object are converging and sufficiently strong, the objects can be suspended and trapped in mid-air [5] (or other propagation media). The trapping of particles using soundwaves is referred to as acoustic levitation, acoustic trapping, acoustic tweezers or acoustophoresis.

Acoustic trapping can be used to hold particles of various materials and sizes. This is in contrasts with optical trapping in which the trapped objects have to be of micrometric scale and the material should be optically transparent or dielectric [6]. Acoustic trapping is also more efficient in terms of input power to exerted forces [7]. Other types of contactless trapping, such as electrostatic levitation [8] requires a close-loop control system and the range of object materials is also limited, aerodynamic levitation [9] stirs and disturbs the samples. Magnetic levitation is a popular method to hold objects in mid-air [10] however it works only on ferromagnetic materials; diamagnetic materials can also be employed [11,12] but due to the much weaker diamagnetic effect, the required amount of power is only accessible to a couple of research laboratories.

The flexibility of acoustic levitation in mid-air has made it a valuable apparatus for containerless transportation [13,14], pharmaceutics [15], nano-assemblies [16], the levitation of biological samples [17], little animals [18,19] and food [20]. Acoustic levitation of liquid droplets can be employed to explore novel liquid dynamics [21], measure surface tension [22,23] or rheological properties [24]. Other applications are the formation of suspended ice flakes [25], growing crystals in liquid metals [26], evaporation of solutions [27], investigation of phase transitions [28], the fast crystallization [29] or ionization [30] of samples, and the creation of bubbles for coverings [31]. Samples held with acoustic levitation are not in physical contact with a container, this provides benefits in mass [32] and Raman [33] spectroscopy, e.g. in

algae [34] or blood cells [17] characterization. In general, acoustic levitation is a helpful and adaptable tool in biomaterials research [35], chemistry [36] and enables lab-on-a-drop procedures [37].

Single-axis levitators [38] are the most typical device for producing acoustic traps. They are compossed of an acoustic emitter and a reflector opposed to it. A standing wave is generated between the emitter and the reflector. The nodes of the standing wave act as an acoustic traps for spherical particles smaller than half-wavelength and with positive acoustic contrast (i.e. the acoustic impadence of the particle is larger than that of the propagation medium). When the medium is water-based, it is also posible to have particles with negative contrast, in this case, the particles go to the anti-nodes [39]. A simple single-axis levitator is presented in Figure 1 as well as the simulated amplitude field that generates and the forces that exert on a 1mm diameter spherical particle.

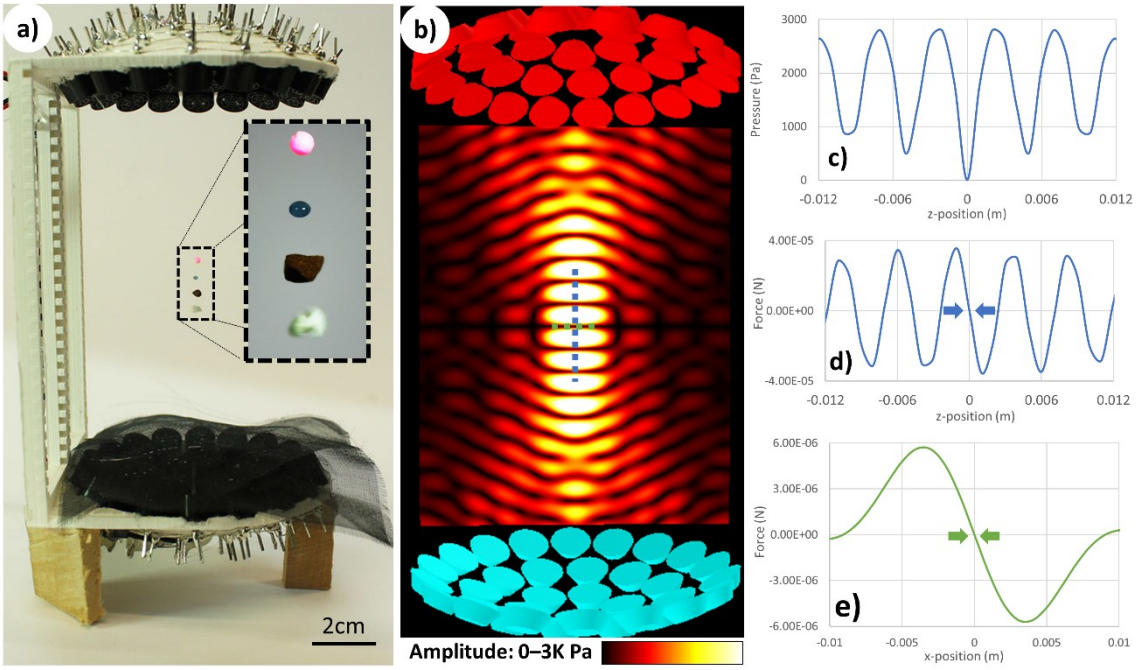


**Figure 1.** a) TinyLev, a single-axis levitator, trapping plastic, water, soil and paper. b) the amplitude pressure field generate by the levitator. c) the amplitude pressure distribution across the vertical axis z. d) the force acting on a particle of 1mm diameter depending on its position along the z-axis and (e) x-axis. Note that both forces are converging towards the center.

Standing waves are the most common method to trap particles given its trapping strength but present some limitations such as particle size (it has to be smaller than half-wavelength) and spherical shape. Some of these limitations have been overcame in the past years. Particles larger than half-wavelength can be levitated close to an emitter using near-field levitation [40,41]. Also, special types of acoustic vortices can trap objects larger than the wavelength in the far-field [42,43] however they require high-

power and only very light objects have been trapped. Non-spherical particles can be steadily trapped using the acoustic lock technique [44] but extra control on the emission of the fields is needed.

Apart from standing-waves, acoustic beams emitted from a single-sided device are capable of trapping particles in three dimensions [45,46,7,47], these beams are also referred to as tractor beams since they can attract particles towards the source, i.e. generate negative forces along the propagation direction of the beam. However, complex equipment or high-power is required for generating functional tractor beams. Consequently, standing-wave trapping remains as the most common method to trap samples in mid-air. A more detailed description of the acoustic levitaiton methods can be found in these reviews [48,49].

We have covered the trapping of one or a series of particle along the static nodes of a standing-wave, but it is also possible to generate multiple standing waves with nodes at user specified positions. Multi-emitter arrays arranged in an opposed configuration enable the trapping of multiple particles that can be moved independently, these traps are named Holographic Acoustic Tweezers [50].

In the second section of the chapter, we will review the main models employed to calculate the acoustic field genarated by acoustic levitators and how to determine the exerted forces on the objects that are contained in these fields. In the third section, the most common configurations used for standing-waves levitators are reviewed.

## 2. PRINCIPLE GOVERNING EQUATIONS

In this section, we describe the most common models used to calculate the generated acoustic field by an acoustic emitter, and the forces that this field exerts on objects. When the models operate in the frequency domain at a single-frequency, the acoustic pressure $(p)$ is represented as a complex scalar field: the magnitude represents the amplitude in pascals and the argument is the phase in radians. When the models operate in the time-domain, the pressure is a real scalar field. The particle velocity of the medium $(\boldsymbol{v})$ is a vector field that also appears in the calculations, it can be obtained from the model or as the gradient of the pressure.

Other terms that regularly appear in the models are: total, incident and scattered fields. The incident field is the acoustic field generated by the emitters into the free-space, i.e.

no reflectors or obstacles that affect the emitted waves are in the domain. The total field is the pressure distribution that exists in the space when all the elements that affect the wave are considered, in theory the total field is what gets measured in the experiments. The total, indecent and scattered fields are linear both for pressure and velocity under the assumptions of most of the models. Consequently, total = incident + scattered, by having two of the fields the other field can be obtained, some models calculate just the incident field whereas other models determine the scattered or directly the total field.

### 2.1. Generated Acoustic Field

**Free-field piston source.**

This is one of the simplest models to calculate an incident field generated by one or multiple emitters which are shapped or can be approximated as circular radiating pistons. The model is only valid for the far-field of the emitters, this is usually not a problem since levitation occurs in the far-field. In general, this method is not suitable for calculating models with complex reflecting geometry or particles which are larger than half-wavelength since the scaterred field would have a significant magnitude. Simple planar reflectors can be approximated by mirroring the emitters and adding an attenuation coefficient depending on the material. On the other hand, this method is fast and can run in real time for hundreds of emitters [51].

The complex acoustic pressure $p$ at point $\boldsymbol{r}$ due to a piston source emitting at a single frequency can be modelled as [52]:

$$p(\boldsymbol{r}) = P_0 V \frac{D_f(\theta)}{d} e^{i(\varphi + kd)}$$

Where $P_0$ is a constant that defines the transducer output efficiency and $V$ is the excitation signal peak-to-peak amplitude. $D_f$ is a far-field directivity function that depends on the angle $\theta$ between the piston normal and the the point $\boldsymbol{r}$. The directivity function of a piston source can be expressed as $D_f = 2J_1(ka \sin\theta)/ka \sin\theta$ , where $J_1$ is a first order Bessel function of the first kind and $a$ is the radius of the piston [53]. This directivity function can be simplified as $D_f = sinc(ka \sin\theta)$ . Other geometries such as square or line transducers can be aproximated with other directivity functions. The term $1/d$ accounts for divergence, where $d$ is the propagation distance in free

space. $k = 2\pi/\lambda$ is the wavenumber and $\lambda$ is the wavelength. $\varphi$ is the emitting phase of the source.

The total acoustic field ($P$) generated by $N$ transducers is the addition of the individual fields, i.e. $P = \sum_{j=1}^{N} p_j$. To characterize a transducer, the constant ($P_0$) and the piston radius ($a$) are needed; the constants for different transducers can be found in the supplementary information of [54]. For instance, the commonly used MA40S4S (Murata Electronics, Japan) have these values: $a$=4.5mm and $P_0 = 0.17 \frac{Pascal\ x\ Meter}{Volt}$

**Scattered Field form a Particle using Spherical Harmonics**

If the particle is larger than half-wavelength, the generated scatered field would influence the simulations, thus modelling only the incident field may not be sufficient. A way of obtaining the scattered field is using spherical harmonics. Here, we explain the overall method but complete solutions are described in [55,42,56].

The linearity of the acoustic fields allows us to represent the incident $p_{in}$ and scattered $p_{sc}$ fields as series of spherical harmonics $Y_n^m(\Omega)$ (where $\Omega = (\theta, \varphi)$ is the solid angle in spherical coordinates), with modal amplitudes $A_n^m$ and $T_n^m$. The incident field can be expressed as:

$$p_{in}(\boldsymbol{r}) = p_0 \sum_{n=0}^{\infty} \sum_{m=-n}^{n} j_n(kr) A_n^m Y_n^m(\Omega).$$

And the scattered field as:

$$p_{sc}(\boldsymbol{r}) = p_0 \sum_{n=0}^{\infty} \sum_{m=-n}^{n} h_n^{(1)}(kr) T_n^m A_n^m Y_n^m(\Omega).$$

Where $j_n$ ($h_n^{(1)}$) is a Hankel function. The scattering coefficients $T_n^m$ characterise the properties of the scattering particle: they depend on the particle shape, the boundary conditions and the internal properties of the particle as well as on the frequency. For a rigid sphere [57] of radius $a$, the scattering coefficient is given by $T_n^m = -j_n'(ka)/h_n^{(1)'}(ka)\delta_{nm}$, where $'$ denotes differentiation and $\delta_{nm}$ is the Kronecker's delta. Other coefficients can be obtained for non-solid particles of different shapes.

Using the orthogonality property of the spherical harmonics, the expansion coefficients $A_n^m$ (often called beam-shape coefficients) can be obtained as:

$$p_0 A_n^m = \frac{1}{j_n(kR)} \iint_\Omega p_{in}(R,\Omega)\, Y_n^{m*}(\Omega)\mathrm{d}\Omega,$$

where $R$ is the radius of the spherical volume in which the incident field $p_{in}$ propagates; this volume contains the trapped object.

The incident and scatered field in the far field ($r \to \infty$), can be expressed as:

$$p_{in} \approx \frac{p_0}{kr} \sum_{n=0}^{\infty} \sum_{m=-n}^{n} \sin(kr - n\pi/2)\, A_n^m Y_n^m(\Omega)\,;$$

$$p_{sc} \approx \frac{p_0}{\mathrm{i}kr} \mathrm{e}^{\mathrm{i}kr} \sum_{n=0}^{\infty} \sum_{m=-n}^{n} \mathrm{i}^{-n} A_n^m T_n^m Y_n^m(\Omega).$$

This method requires the calculation of the incident field, for instance using the previously described free-field piston model. The analytical scaterred field generated by the particle can be added to the incident field to get the total field. This model cannot capture the reflections caused by reflectors of complex shapes or other objects affecting the field apart from the levitated object.

**Numerical Methods**

Numerical methods are preferred to calculate the acoustic field when the domain to be simulated contains complex geometry, for instance hollow tubes of different lengths [46,58], a levitated particle of complex shape [44], or a curved reflector [59]. In general, these methods take more time to execute than the analytic methods and are less precise but are the only feasible alternative when there are complex geometries in the domain.

One of the simplest numerical methods are the Finite Differences Time Domain (FDTD) simulations in which the domain is divided into a stagged grid for pressure and velocity [60]. More genereal Finite Elements modelling is also possible [61]. If the propagation is on liquids then it is sufficient to use a scalar pressure and velocity vector, but on solids a complete simulations requires the use of stress tensors [62].

The most employed numerical method on the literature is the boundary elements from the COMSOL package. It allows for irregulate meshes of different densities thus giving a good compromise between accuracy and execution time.

If the trapped particle is smaller than half-wavelength, it could be posible to simulate the field without the particle inside the levitator. The obtained field could be used to

calculate forces, independently from the type and position of the particle. However, for large particles and resonant levitators, a simulaiton with the particle inside is recommended.

### 2.2. Acoustic Radiation Force

The acoustic field will exert a radiation force on the particles contained inside the field. There are other effects such as thermal or viscous contributions [63] but here we focus on the radiation force since it is the dominant force for particles that are large in comparison to the viscous layer [1].

Two methods are presented, one is the Gork'ov potential which is a simple method to calculate the force acting on a particle. The Gork'ov potential only requires the incident field to determine the forces acting on a particle but it assumes that the particle is much smaller than the wavelength, spherical and rigid. On the other hand, the flux integral is a more general method to calculate the force acting on an arbitrary-shaped object of any size, it is a more complex approach since it requires the calculation of the total field and an integration over the surface of a sphere that encloses the trapped object.

#### Gork'ov potential

Gork'ov derived a simplification of the forces acting on a particle when it is in an acoustic field [3]. A modern and more detailed derivation of the Gork'ov potential was described by Bruus [1]. To calculate the force exerted on a sphere significantly smaller than the wavelength due to a complex pressure field, the negative gradient of the Gor'kov potential can be used $\boldsymbol{F} = -\boldsymbol{\nabla} U$ where the potential $U$ can be defined in terms of the incident pressure:

$$U = 2K_1(|p|^2) - 2K_2(|p_x|^2 + |p_y|^2 + |p_z|^2)$$

$$K_1 = \frac{1}{4}V\left(\frac{1}{c_0^2\rho_0} - \frac{1}{c_s^2\rho_s}\right)$$

$$K_2 = \frac{3}{4}V\left(\frac{\rho_0 - \rho_s}{\omega^2\rho_0(\rho_0 + 2\rho_s)}\right)$$

where $V$ is the volume of the spherical particle, $\omega$ is the frequency of the emitted waves, $\rho$ is the density and $c$ is the speed of sound (subscripts *0* and *s* referring to the host medium and the particle material respectively). $p$ is the complex pressure and $p_x, p_y, p_z$ are its spatial derivates over *x*, *y* and *z*. $U$ can also be expressed as a function of the

pressure ($p$) and the velocity ($\boldsymbol{v}$) but since the velocity can be obtained as the gradient of the pressure [1], we consider this expression more compact. In any case, the fields should be calculated without the particle in the model.

**Radiation Flux Integral.**

The radiation force acting on an object can be obtained by the integration of the momentum fluxes over an enclosing sphere. If the total field is given in the frequency domain, the second-order approximation of the radiation force can be expressed as [64]:

$$\boldsymbol{F} = \iint_S \left\{\left(\frac{1}{4}\rho|\boldsymbol{v}|^2 - \frac{1}{4\rho c^2}|p|^2\right)\boldsymbol{n} - \frac{1}{2}\rho\mathrm{Re}[\boldsymbol{v}^*(\boldsymbol{v}\cdot\boldsymbol{n})]\right\}\mathrm{d}S,$$

where $p$ and $\boldsymbol{v}$ are the complex pressure and particle velocity due to an acoustic field with time dependence $\exp(-\mathrm{i}\omega t)$, $S$ is a surface, $\boldsymbol{n}$ is the normal to the surface enclosing the system, and $*$ is the complex conjugation.

If the pressure and velocity fields are in the time domain the expression is as follows [61,56,65]:

$$\boldsymbol{F} = \iint_S -\frac{1}{2\rho c^2}\langle p^2\rangle + \frac{1}{2}\rho\langle v^2\rangle - \rho\langle(\boldsymbol{v}\boldsymbol{n})\cdot\boldsymbol{v}\rangle\mathrm{d}\boldsymbol{a},$$

With $\langle\,\rangle$ representing the time average.

**3. Levitator Geometries**

The most employed configuration for acoustic levitators is the single-axis levitator [38] which can be divided into two main categories. On the one hand, a standing-wave can be generated by an emitter and an opposed reflector; the shape, distance and material of the reflector has a fundamental role on the efficiency. On the other hand, two opposed emitters can be employed to add extra acoustic power and versatility [66].

Another classification attends to the resonant nature of the levitator, there are non-resonant [66] and resonant [67] levitators. These division is more like a continuous spectrum in which the levitators have a certain degree of resonance. Resonant devices are more efficient (i.e. larger trapping forces per input power) but are harder to tune due to changes in atmospheric temperature, humidity and barometric pressure. Non-resonant levitators are simpler to use since they do not need tuning but are not as efficient. In general, a low ratio of distance between the opposed elements and their emission

aperture leads to a highly resonant device, whereas levitators with small radiating surfaces and large separations will be less resonant.

Langevin horns are a common design for the emitters, they are devices made of piezoelectric disks clamped between a backing material and a resonating horn [68]. They can operate at high-voltages (typically 100-1000 V) and generate high acoustic pressures with a single emitter; however, they have some disadvantages. Is difficult to tune Langevin horns to a specific resonant frequency, Weber *et al* [66] built dozens of horns to obtain two horns with a sufficiently close resonant frequency. Also, the high-voltage required to operate the horns could be dangerous. Furthermore, Langevin horns typically heat up over time and shift their resonant frequency. One alternative is to employ small ultrasonic transducers used predominantly in distance ranging applications. They are capable of outputing enough power to obtain levitation of samples of up to 7 g/cm$^3$ [54]. To summarize, the emitters used for levitation are either Langevin horns or off-the-shelf rangefinding transducers.

An example of different standing-wave levitator configurations is shown in Figure 2, each of the arrangements is described with more detail in the following subsections.

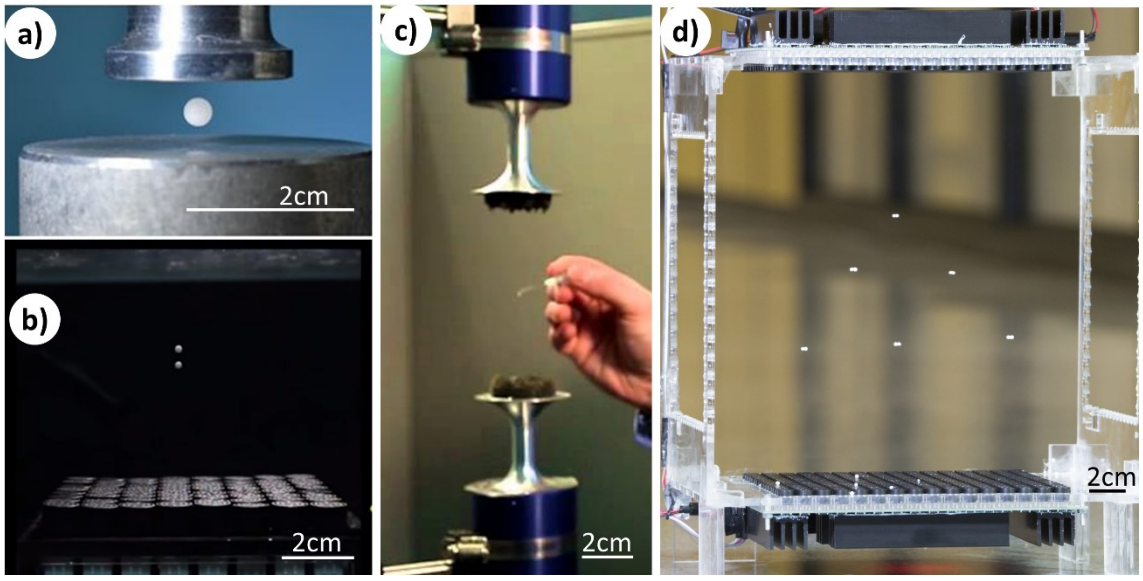


**Figure 2.** a) Emitter on top and reflector on the bottom, Figure extracted from [48]. b) phased-array on the bottom and reflector on top. c) two opposed emitters, Figure extract from [66] d) two opposed phased-arrays.

### Single-emitter and a reflector.

In this configuration, an emitter generates an acoustic wave that reflects on a solid element placed in front of it at a certain distance. The reflected wave adds to the emitted wave and create a standing wave.

Most of the times, the emitter is a high-power Langevin transducer [68]. An emitter with large diameter of the radiator leads to more stable levitation [69,70,71], therefore Langevin horns for acoustic levitation usually have special designs with a large diameter of the radiation surface (i.e. horn shape).

Considerable research has been conducted on the shape and size of the reflector. A concave reflector leads to stronger acoustic traps than the common planar reflector [59,70,71]. Using a concave emitter increased significantly the efficiency of the levitators by locally concentrating the acoustic energy [67]. To improve the adaptability of emitter-reflector levitators, a morphing reflector made of water or elastic materials was employed [72,73]. It is also possible to enclose the levitator with a tube to improve the performance [74].

When the levitator is resonant, a change in temperature can detune the levitator and reduce the trapping strength [75]. Similarly, introducing large samples in the levitator can shift the resonant frequency [76] and create instabilities [77]. Also, non-linear behaviors such as second harmonic generation can reduce the trapping force [78].

**Two opposed emitters.**

Instead of using a passive reflector to create the standing wave, another possibility is to use two opposed emitters. This allows to put more direct acoustic power and also to move the samples along the axis by changing the phase [38]. Given the extra acoustic power and phase adjustment these systems can be used to create non-resonant levitators which are in general more versatile [66]. Using this approach, a levitator is more robust to external conditions (e.g. temperature, humidity or barometric preasure), being able to operate at temperatures rangin from −40 to +40 °C and requiring less calibration of the separation between the emitters.

**Phased-array and a reflector**

Phased arrays are an assortment of transducers that transmit or receive using user defined phase or time delays. They are commonly used in radar [79] or sonar [80] given their ability to dynamically steer and shape the beam. Phased-arrays are employed also in standing-wave levitators [7,54,51] for their capability of refocusing and shifting the standing waves, thus moving the trapped particles dynamically. However, the trapped

particles cannot be moved perpendicularly to the reflector, they can only be moved in a plane parallel to it.

The traps can be moved without displacing the levitator by adjusting the phase of the emitters. A common configuration is to use a phased-array opposed to a parallel reflector. The principle of operation is the same as the emitter-reflector but this time the emitted focal point can be moved dynamically; it is also possible to create multiple focal points. These focal points reflect on the opposed reflector and create standing waves. This has been shown for manipulating multiple samples and merging them in mid-air [13,82,83].

**Two opposed phased-arrays.**

Using two-opposed phased-arrays is possible to create standing waves that also shift their nodes perpendicularly to the arrays. Firstly, it was shown that with two-opposed arrays 3D positioning of one particle was possible [81], and then that the individual positioning of multiple particles can be achieved [50]. An iterative backpropagation (IB) algorithm is empoyed to generate multiple functional traps using arbitrary arrangements of transducers [50]. Two opposed 256-emitter phased-arrays are manipulating individually 6 millimetric particles in Figure 3.

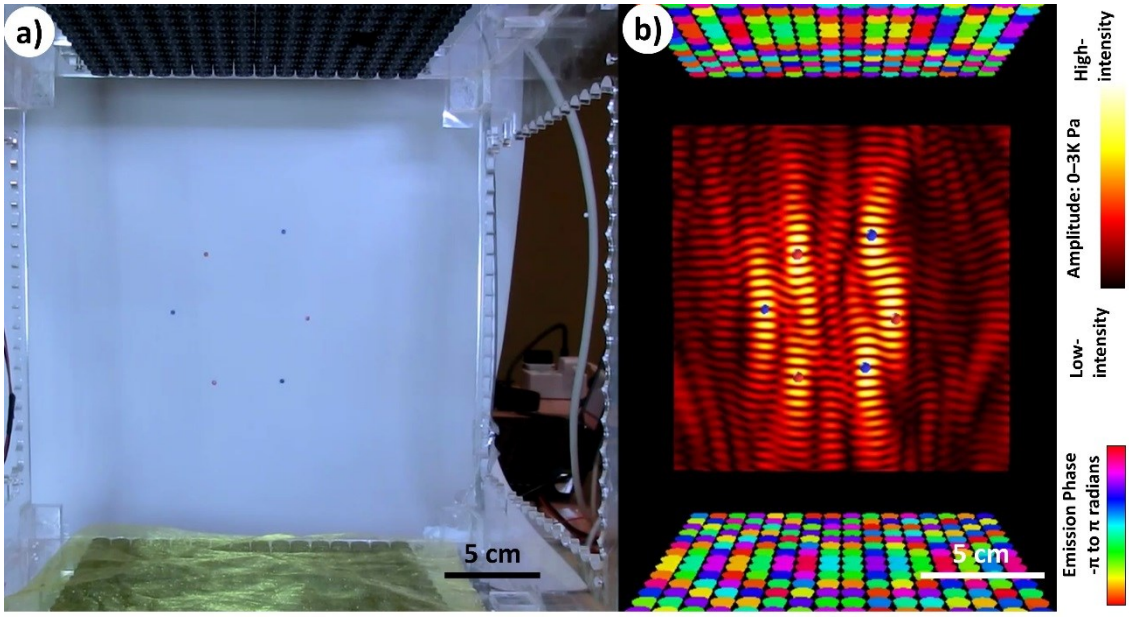


**Figure 3.** a) Two opposed arrays made of 16x16 ultrasonic transducers operating at 40 kHz are trapping 6 spherical particles made of Styrofoam. b) the simulated amplitude pressure field as well as the emission phases of the transducers.

When designing standing-wave levitators made of phased-arrays it must be taken into account that the maximum trapping forces are achieved with emitting arrays that satisfy

Nyquist sampling [50] (i.e. the emitters are half-wavelength in size) and an emission phase discretisation of $\pi/8$ radians [51]. That is, for standing-wave trapping applications there is no increase in the trapping strength when having emitters smaller than half-wavelength or creating electronics that support phase resolutions of more than 16 divisions per period.

### Other geometries

There are other geometries apart from the ones presented here: four orthognal emitters [84] or arrays [85], emitters arranged in a heptagon [86], or in a circle [87,88,89]. Also, instead of using phased-arrays, the requiered phase modulations can be achieved using metamaterials [46,58,39] or a mix of matamaterials and phased-arrays [90]. Although this method has less complexity (regarding hardware and cost) it only enables static levitation or restricted movement.

## 2.3. Conclusion

An acoustic standing wave with enough pressure amplitude will trap particles smaller than half-wavelength and of positive acoustic contrast (the particle has more acoustic impedance than the medium). This is the basic principle behind acoustic levitation and enables multiple applications in contactless manipulation of samples for spectroscopic analysis of materials, amorphous crystallization of solutions or characterization of liquid properties.

Multiple levitator configurations exist to generate standing waves of high-amplitude. Single-axis levitators made of an emitter and an opposed reflector are a simple way to hold samples in mid-air. More complex devices based on phased-arrays allow the manipulation of multiple particles independently and thus enable more complex protocols such as mixing of samples. Despite the advances on acoustic trapping with vortices or tractor beams, standing waves remain as the main method to trap particles in mid-air.

## REFERENCES


1. Bruus, H., “Acoustofluidics 7: The acoustic radiation force on small particles,” Lab Chip 12(6), 1014–1021 (2012). https://doi.org/10.1039/c2lc21068a9.
2. Doinikov, A. A., “On the radiation pressure on small spheres,” J. Acoust. Soc. Am. 100(2), 1231–1233 (1996). https://doi.org/10.1121/1.41596915.
3. Gorkov, L. P., “Forces acting on a small particle in an acoustic field within an

ideal fluid," Dokl. Akad. Nauk SSSR 140(1), 88 (1961).18.
4. King, L. V., "On the acoustic radiation pressure on spheres," Proc. R. Soc. A 147(861), 212–240 (1934). https://doi.org/10.1098/rspa.1934.0215
5. Brandt, E. H., "Acoustic physics: Suspended by sound," Nature 413(6855), 474–475 (2001). https://doi.org/10.1038/35097192
6. Neuman, K. C. and Block, S. M., "Optical trapping," Rev. Sci. Instrum. 75(9), 2787–2809 (2004). https://doi.org/10.1063/1.1785844
7. Marzo, A., Seah, S. A., Drinkwater, B. W., Sahoo, D. R., Long, B., and Subramanian, S., "Holographic acoustic elements for manipulation of levitated objects," Nat. Commun. 6, 8661 (2015). https://doi.org/10.1038/ncomms9661
8. Mauro, N. A. and Kelton, K. F., "A highly modular beamline electrostatic levitation facility, optimized for in situ high-energy x-ray scattering studies of equilibrium and supercooled liquids," Rev. Sci. Instrum. 82(3), 035114 (2011).
9. Yarin, A. L., Brenn, G., Keller, J., Pfaffenlehner, M., Ryssel, E., and Tropea, C., "Flowfield characteristics of an aerodynamic acoustic levitator," Phys. Fluids 9(11), 3300–3314 (1997). https://doi.org/10.1063/1.869444
10. El Hajjaji, A. and Ouladsine, M., "Modeling and nonlinear control of magnetic levitation systems," IEEE Trans. Ind. Electron. 48(4), 831–838 (2001). https://doi.org/10.1109/41.937416
11. Geim, A. K., Simon, M. D., Boamfa, M. I., and Heflinger, L. O., "Magnet levitation at your fingertips," Nature 400(6742), 323 (1999). https://doi.org/10.1038/22444
12. Berry, M. V. and Geim, A. K., "Of flying frogs and levitrons," Eur. J. Phys. 18(4), 307 (1997). https://doi.org/10.1088/0143-0807/18/4/012
13. Foresti, D., Nabavi, M., Klingauf, M., Ferrari, A., and Poulikakos, D., "Acoustophoretic contactless transport and handling of matter in air," Proc. Natl. Acad. Sci. U. S. A. 110(31), 12549–12554 (2013). https://doi.org/10.1073/pnas.130186011019.
14. Kozuka, T., Yasui, K., Tuziuti, T., Towata, A., and Iida, Y., "Noncontact acoustic manipulation in air," Jpn. J. Appl. Phys., Part 1 46(7S), 4948(2007). https://doi.org/10.1143/jjap.46.4948
15. Benmore, C. J. and Weber, J. K. R., "Amorphization of molecular liquids of pharmaceutical drugs by acoustic levitation," Phys. Rev. X 1(1), 011004 (2011). https://doi.org/10.1103/physrevx.1.011004
16. Seddon, A. M., Richardson, S. J., Rastogi, K., Plivelic, T. S., Squires, A. M., and Pfrang, C., "Control of nanomaterial self-assembly in ultrasonically levitated droplets," J. Phys. Chem. Lett. 7(7), 1341–1345(2016). https://doi.org/10.1021/acs.jpclett.6b00449
17. Puskar, L., Tuckermann, R., Frosch, T., Popp, J., Ly, V., McNaughton, D., and Wood, B. R., "Raman acoustic levitation spectroscopy of red blood cells and Plasmodium falciparum trophozoites," Lab Chip 7(9), 1125–1131 (2007). https://doi.org/10.1039/b706997a
18. Sundvik, M., Nieminen, H. J., Salmi, A., Panula, P., and Hæggström, E., "Effects of acoustic levitation on the development of zebrafish, Danio rerio, embryos," Sci. Rep. 5, 13596 (2015). https://doi.org/10.1038/srep1359652.
19. Xie, W. J., Cao, C. D., Lü, Y. J., Hong, Z. Y., and Wei, B., "Acoustic method for levitation of small living animals," Appl. Phys. Lett. 89(21), 214102 (2006). https://doi.org/10.1063/1.2396893
20. Vi, Chi Thanh, et al. "Tastyfloats: A contactless food delivery system." Proceedings of the 2017 ACM International Conference on Interactive Surfaces

and Spaces. ACM, 2017.
21. Trinh, E. and Wang, T. G., “Large-amplitude free and driven drop-shape oscillations: Experimental observations,” J. Fluid Mech. 122, 315–338 (1982). https://doi.org/10.1017/s0022112082002237
22. Tian, Y., Holt, R. G., and Apfel, R. E., “A new method for measuring liquid surface tension with acoustic levitation,” Rev. Sci. Instrum. 66(5), 3349–3354 (1995). https://doi.org/10.1063/1.1145506
23. Trinh, E. H., Marston, P. L., and Robey, J. L., “Acoustic measurement of the surface tension of levitated drops,” J. Colloid Interface Sci. 124(1), 95–103 (1988). https://doi.org/10.1016/0021-9797(88)90329-3
24. Tian, Y., Holt, R. G., and Apfel, R. E., “Investigation of liquid surface rheology of surfactant solutions by droplet shape oscillations: Experiments,” J. Colloid Interface Sci. 187(1), 1–10 (1997). https://doi.org/10.1006/jcis.1996.4698
25. Bauerecker, S. and Neidhart, B., “Formation and growth of ice particles in stationary ultrasonic fields,” J. Chem. Phys. 109(10), 3709–3712 (1998). https://doi.org/10.1063/1.476971
26. Xie, W. J., Cao, C. D., Lü, Y. J., and Wei, B., “Eutectic growth under acoustic levitation conditions,” Phys. Rev. E 66(6), 061601 (2002). https://doi.org/10.1103/physreve.66.061601
27. Yarin, A. L., Brenn, G., and Rensink, D., “Evaporation of acoustically levitated droplets of binary liquid mixtures,” Int. J. Heat Fluid Flow 23(4), 471–486 (2002). https://doi.org/10.1016/s0142-727x(02)00142-x
28. Ermoline, A., Schoenitz, M., Hoffmann, V. K., and Dreizin, E. L., “Experimental technique for studying high-temperature phases in reactive molten metal based systems,” Rev. Sci. Instrum. 75(12), 5177–5185(2004). https://doi.org/10.1063/1.1819011
29. Cao, H. L., Yin, D. C., Guo, Y. Z., Ma, X. L., He, J., Guo, W. H., Xie, X.-Z., and Zhou, B. R., “Rapid crystallization from acoustically levitated droplets,” J. Acoust. Soc. Am. 131(4), 3164–3172 (2012). https://doi.org/10.1121/1.3688494
30. Stindt, A., Albrecht, M., Panne, U., and Riedel, J., “CO2 laser ionization of acoustically levitated droplets,” Anal. Bioanal. Chem. 405(22), 7005–7010 (2013). https://doi.org/10.1007/s00216-012-6500-y
31. Zang, Duyang, et al. "Inducing drop to bubble transformation via resonance in ultrasound." Nature communications 9.1 (2018): 3546.
32. Westphall, M. S., Jorabchi, K., and Smith, L. M., “Mass spectrometry of acoustically levitated droplets,” Anal. Chem. 80(15), 5847–5853 (2008). https://doi.org/10.1021/ac800317f
33. Santesson, S., Johansson, J., Taylor, L. S., Levander, I., Fox, S., Sepaniak, M., and Nilsson, S., “Airborne chemistry coupled to Raman spectroscopy,” Anal. Chem. 75(9), 2177–2180 (2003). https://doi.org/10.1021/ac026302w
34. Wood, B. R., Heraud, P., Stojkovic, S., Morrison, D., Beardall, J., and McNaughton, D., “A portable Raman acoustic levitation spectroscopic system for the identification and environmental monitoring of algal cells,” Anal. Chem. 77(15), 4955–4961 (2005). https://doi.org/10.1021/ac050281z
35. Weber, R. J., Benmore, C. J., Tumber, S. K., Tailor, A. N., Rey, C. A., Taylor, L. S., and Byrn, S. R., “Acoustic levitation: Recent developments and emerging opportunities in biomaterials research,” Eur. Biophys. J. 41(4), 397–403 (2012). https://doi.org/10.1007/s00249-011-0767-3
36. Santesson, S. and Nilsson, S., “Airborne chemistry: Acoustic levitation in chemical analysis,” Anal. Bioanal. Chem. 378(7), 1704–1709 (2004).

https://doi.org/10.1007/s00216-003-2403-2
37. Priego-Capote, F. and de Castro, L., “Ultrasound-assisted levitation: Lab-on-a-drop,” TrAC, Trends Anal. Chem. 25(9), 856–867 (2006). https://doi.org/10.1016/j.trac.2006.05.014
38. Whymark, R. R., “Acoustic field positioning for containerless processing,” Ultrasonics 13(6), 251–261 (1975). https://doi.org/10.1016/0041-624x(75)90072-4
39. Melde, Kai, et al. "Holograms for acoustics." Nature 537.7621 (2016): 518.
40. Ueha, Sadayuki, Yoshiki Hashimoto, and Yoshikazu Koike. "Non-contact transportation using near-field acoustic levitation." Ultrasonics 38.1-8 (2000): 26-32.
41. Andrade, Marco AB, Anne L. Bernassau, and Julio C. Adamowski. "Acoustic levitation of a large solid sphere." Applied Physics Letters 109.4 (2016): 044101.
42. Marzo, Asier, Mihai Caleap, and Bruce W. Drinkwater. "Acoustic virtual vortices with tunable orbital angular momentum for trapping of mie particles." Physical review letters 120.4 (2018): 044301.
43. Inoue, Seki, et al. "Acoustic macroscopic rigid body levitation by responsive boundary hologram." arXiv preprint arXiv:1708.05988 (2017).
44. Cox, L., et al. "Acoustic lock: Position and orientation trapping of non-spherical sub-wavelength particles in mid-air using a single-axis acoustic levitator." Applied Physics Letters 113.5 (2018): 054101.
45. Démoré, Christine EM, et al. "Acoustic tractor beam." Physical review letters 112.17 (2014): 174302.
46. Marzo, A., et al. "Realization of compact tractor beams using acoustic delay-lines." Applied Physics Letters 110.1 (2017): 014102.
47. Baresch, Diego, Jean-Louis Thomas, and Régis Marchiano. "Observation of a single-beam gradient force acoustical trap for elastic particles: acoustical tweezers." Physical review letters 116.2 (2016): 024301.
48. Andrade, Marco AB, Nicolás Pérez, and Julio C. Adamowski. "Review of Progress in Acoustic Levitation." Brazilian Journal of Physics 48.2 (2018): 190-213.
49. Drinkwater, Bruce W. "Dynamic-field devices for the ultrasonic manipulation of microparticles." Lab on a Chip 16.13 (2016): 2360-2375.
50. Marzo, Asier, and Bruce W. Drinkwater. "Holographic acoustic tweezers." Proceedings of the National Academy of Sciences 116.1 (2019): 84-89.
51. Marzo, Asier, Tom Corkett, and Bruce W. Drinkwater. "Ultraino: An open phased-array system for narrowband airborne ultrasound transmission." IEEE transactions on ultrasonics, ferroelectrics, and frequency control 65.1 (2017): 102-111.
52. H. T. O’Neil, "Theory of focusing radiators", J. Acoust. Soc. Amer., vol. 21, no. 5, pp. 516-526, 1949.
53. Aarts, Ronald M., and Augustus JEM Janssen. "On-axis and far-field sound radiation from resilient flat and dome-shaped radiators." The Journal of the Acoustical Society of America 125.3 (2009): 1444-1455.
54. Marzo, Asier, Adrian Barnes, and Bruce W. Drinkwater. "TinyLev: A multi-emitter single-axis acoustic levitator." Review of Scientific Instruments 88.8 (2017): 085105.
55. Sapozhnikov, Oleg A., and Michael R. Bailey. "Radiation force of an arbitrary acoustic beam on an elastic sphere in a fluid." The Journal of the Acoustical

Society of America 133.2 (2013): 661-676.
56. Baresch, Diego, Jean-Louis Thomas, and Régis Marchiano. "Three-dimensional acoustic radiation force on an arbitrarily located elastic sphere." The Journal of the Acoustical Society of America 133.1 (2013): 25-36.
57. Faran Jr, James J. "Sound scattering by solid cylinders and spheres." The Journal of the acoustical society of America 23.4 (1951): 405-418.
58. Memoli, Gianluca, et al. "Metamaterial bricks and quantization of meta-surfaces." Nature communications 8 (2017): 14608.
59. Oran, W. A., Berge, L. H., and Parker, H. W., "Parametric study of an acoustic levitation system," Rev. Sci. Instrum. 51(5), 626–631 (1980). https://doi.org/10.1063/1.1136268
60. A. Allen and N. Raghuvanshi, "Aerophones in flatland: Interactive wave simulation of wind instruments," ACM Trans. Graphics (TOG) 34(4), 134 (2015). https://doi.org/10.1145/2767001
61. Glynne-Jones, Peter, et al. "Efficient finite element modeling of radiation forces on elastic particles of arbitrary size and geometry." The Journal of the Acoustical Society of America 133.4 (2013): 1885-1893.
62. Tanikaga, Yoko, T. Sakaguchi, and Y. Watanabe. "A study on analysis of intracranial acoustic wave propagation by the finite difference time domain method." Proceedings of Forum Acusticum, Sevilla. Vol. 4. No. 4.1. 2002.
63. Settnes, Mikkel, and Henrik Bruus. "Forces acting on a small particle in an acoustical field in a viscous fluid." Physical Review E 85.1 (2012): 016327.
64. Westervelt, Peter J. "Scattering of sound by sound." The Journal of the Acoustical Society of America 29.2 (1957): 199-203.
65. Borgnis, F. E. "Acoustic radiation pressure of plane compressional waves." Reviews of Modern Physics 25.3 (1953): 653.
66. Weber, J. K. R., Rey, C. A., Neuefeind, J., and Benmore, C. J., "Acoustic levitator for structure measurements on low temperature liquid droplets," Rev. Sci. Instrum. 80(8), 083904 (2009).
67. Andrade, M. A., Buiochi, F., and Adamowski, J. C., "Finite element analysis and optimization of a single-axis acoustic levitator," IEEE Trans. Ultrason. Ferroelectr. Freq. Control 57(2), 469–479 (2010).
68. Lin, S., "Study on the multifrequency Langevin ultrasonic transducer," Ultrasonics 33(6), 445–448 (1995).
69. Trinh, E. H., "Compact acoustic levitation device for studies in fluid dynamics and material science in the laboratory and microgravity," Rev. Sci. Instrum. 56(11), 2059–2065 (1985).
70. Xie, W. J. and Wei, B., "Parametric study of single-axis acoustic levitation," Appl. Phys. Lett. 79(6), 881–883 (2001). https://doi.org/10.1063/1.139139850.
71. Xie, W. J. and Wei, B., "Dependence of acoustic levitation capabilities on geometric parameters," Phys. Rev. E 66(2), 026605 (2002).
72. Foresti, D., Sambatakakis, G., Bottan, S., and Poulikakos, D., "Morphing surfaces enable acoustophoretic contactless transport of ultrahigh-density matter in air," Sci. Rep. 3, 3176 (2013). https://doi.org/10.1038/srep0317616.
73. Hong, Z. Y., Xie, W. J., and Wei, B., "Acoustic levitation with self-adaptive flexible reflectors," Rev. Sci. Instrum. 82(7), 074904 (2011).
74. Jiang, Hai, et al. "Analysis and experimental study on the effect of a resonant tube on the performance of acoustic levitation devices." AIP Advances 6.9 (2016): 095302.
75. Xie, W. J. and Wei, B., "Temperature dependence of single-axis acoustic

levitation," J. Appl. Phys. 93(5), 3016–3021 (2003).
76. Wen-Jun, X. and Bing-Bo, W., "Resonance shift of single-axis acoustic levitation," Chin. Phys. Lett. 24(1), 135 (2007).
77. Andrade, Marco AB, et al. "Experimental investigation of the particle oscillation instability in a single-axis acoustic levitator." AIP Advances 9.3 (2019): 035020.
78. Andrade, M. A., Ramos, T. S., Okina, F. T., and Adamowski, J. C., "Nonlinear characterization of a single-axis acoustic levitator," Rev. Sci. Instrum. 85(4), 045125 (2014).
79. C. Pell, "Phased-array radars", IEE Rev., vol. 34, no. 9, pp. 363-367, 1988.
80. J. H. G. Ender, A. R. Brenner, "PAMIR—A wideband phased array SAR/MTI system", IEE Proc.-Radar Sonar Navigat., vol. 150, no. 3, pp. 165-172, 2003.
81. Omirou, Themis, et al. "LeviPath: Modular acoustic levitation for 3D path visualisations." Proceedings of the 33rd Annual ACM Conference on Human Factors in Computing Systems. ACM, 2015.
82. Watanabe, Ayumu, Koji Hasegawa, and Yutaka Abe. "Contactless fluid manipulation in air: Droplet coalescence and active mixing by acoustic levitation." Scientific reports 8.1 (2018): 10221.
83. Andrade, Marco AB, Thales SA Camargo, and Asier Marzo. "Automatic contactless injection, transportation, merging, and ejection of droplets with a multifocal point acoustic levitator." Review of Scientific Instruments 89.12 (2018): 125105.
84. Nichols, Madeleine K., et al. "Fabrication of Micropatterned Dipeptide Hydrogels by Acoustic Trapping of Stimulus-Responsive Coacervate Droplets." Small 14.26 (2018): 1800739.
85. Ochiai, Yoichi, Takayuki Hoshi, and Jun Rekimoto. "Pixie dust: graphics generated by levitated and animated objects in computational acoustic-potential field." ACM Transactions on Graphics (TOG) 33.4 (2014): 85.
86. Gesellchen, Frank, et al. "Cell patterning with a heptagon acoustic tweezer–application in neurite guidance." Lab on a Chip 14.13 (2014): 2266-2275.
87. Courtney, Charles RP, et al. "Independent trapping and manipulation of microparticles using dexterous acoustic tweezers." Applied Physics Letters 104.15 (2014): 154103.
88. Seah, Sue Ann, et al. "Correspondence: Dexterous ultrasonic levitation of millimeter-sized objects in air." IEEE transactions on ultrasonics, ferroelectrics, and frequency control 61.7 (2014): 1233-1236.
89. Foresti, Daniele, and Dimos Poulikakos. "Acoustophoretic contactless elevation, orbital transport and spinning of matter in air." Physical review letters 112.2 (2014): 024301.
90. Norasikin, Mohd Adili, et al. "SoundBender: dynamic acoustic control behind obstacles." The 31st Annual ACM Symposium on User Interface Software and Technology. ACM, 2018.